

Article

A Secrecy Transmission Protocol with Energy Harvesting for Federated Learning

Ping Xie¹, Fan Li¹, Ilsun You^{2,*}, Ling Xing¹, Honghai Wu¹ and Huahong Ma¹

¹ School of Information Engineering, Henan University of Science and Technology, Luoyang 471023, China; xieping@haust.edu.cn (P.X.); lifan_12398@163.com (F.L.); xingling_my@163.com (L.X.); honghai2018@haust.edu.cn (H.W.); mhh@haust.edu.cn (H.M.)

² Department of Financial Information Security, Kookmin University, Seoul 02707, Korea

* Correspondence: ilsunu@gmail.com

Abstract: In federated learning (FL), model parameters of deep learning are communicated between clients and the central server. To better train deep learning models, the spectrum resource and transmission security need to be guaranteed. Toward this end, we propose a secrecy transmission protocol based on energy harvesting and jammer selection for FL, in which the secondary transmitters can harvest energy from the primary source. Specifically, a secondary transmitter ST_i is first selected, which can offer the best transmission performance for the secondary users to access the primary frequency spectrum. Then, another secondary transmitter ST_n , which has the best channel for eavesdropping, is also chosen as a friendly jammer to provide secrecy service. Furthermore, we use outage probability (OP) and intercept probability (IP) as metrics to evaluate performance. Meanwhile, we also derive closed-form expressions of OP and IP of primary users and OP of secondary users for the proposed protocol, respectively. We also conduct a theoretical analysis of the optimal secondary transmission selection (OSTS) protocol. Finally, the performance of the proposed protocol is validated through numerical experiments. The results show that the secrecy performance of the proposed protocol is better than the OSTS and OCJS, respectively.

Keywords: energy harvesting; federated learning; intercept probability; outage probability; secrecy transmission protocol



Citation: Xie, P.; Li, F.; You, I.; Xing, L.; Wu, H.; Ma, H. A Secrecy Transmission Protocol with Energy Harvesting for Federated Learning. *Sensors* **2022**, *22*, 5506. <https://doi.org/10.3390/s22155506>

Academic Editor: Wai Lok Woo

Received: 27 June 2022

Accepted: 20 July 2022

Published: 23 July 2022

Publisher's Note: MDPI stays neutral with regard to jurisdictional claims in published maps and institutional affiliations.



Copyright: © 2022 by the authors. Licensee MDPI, Basel, Switzerland. This article is an open access article distributed under the terms and conditions of the Creative Commons Attribution (CC BY) license (<https://creativecommons.org/licenses/by/4.0/>).

1. Introduction

In modern artificial intelligence, federated learning (FL) [1] is one of the most dominant collaborative training paradigms. Compared to traditional and centralized training methods, FL can mitigate the privacy leakage risk of data since the model parameters of clients are only transmitted to a central server in the training process. Most of the modern information and communication technologies [2] can satisfy the transmission of model parameters in the fifth generation (5G) networks [3]. Nevertheless, spectrum resource is essential for the transmission of model parameters in FL. Meanwhile, most of the spectrum resources are assigned by the government. Therefore, the spectrum resource is scarce for transmitting large amounts of information. For this reason, cognitive radio (CR) [4] is a promising technique to raise spectrum efficiency [5]. By integrating the advantages of Internet of Things (IoT) and CR, Cognitive Internet of Things (CIoT) becomes a prevalent network pattern. In CIoT, secondary users (SUs) can transmit information opportunistically without affecting legitimate users [6]. Moreover, resource utilization can be improved through intelligent cooperation [7].

However, active transmissions between clients and the central server in the framework of FL are vulnerable to eavesdropping by illegal users due to the essential nature of broadcast communication and dynamic spectrum access in CIoT. Thereby, how to ensure the transmission security and resist malicious intrusion [8] is a crucial problem in FL. To mitigate this problem, the physical-layer security (PLS) technology is an important

protection mechanism [9–12]. In this direction, Csiszar and Korner [13] improved the security performance and broadcast private messages by leveraging the randomization of stochastic encoding. Tang et al. [14] used a helping interferer to improve the security of transmission. Specifically, the achieving secrecy rate can be also obtained even when the conditions of the destination channel are worse than the wiretap channel. Meanwhile, the perfect secrecy capacity of the multiple-input multiple-output (MIMO) channel was analyzed in [15]. Furthermore, the security performance of a multi-antenna system was also improved in [16,17]. In addition, some studies [18–20] have improved PLS by transmitting artificial noise (AN) to hinder eavesdroppers. Moreover, the confidentiality of legitimate users was also improved by selecting an appropriate friendly jammer to transmit AN [21]. The aforementioned efforts were made for the simple traditional system model; however, how to guarantee the secrecy performance of primary users (PUs) with strict requirements of Quality-of-Service (QoS) remains a key issue.

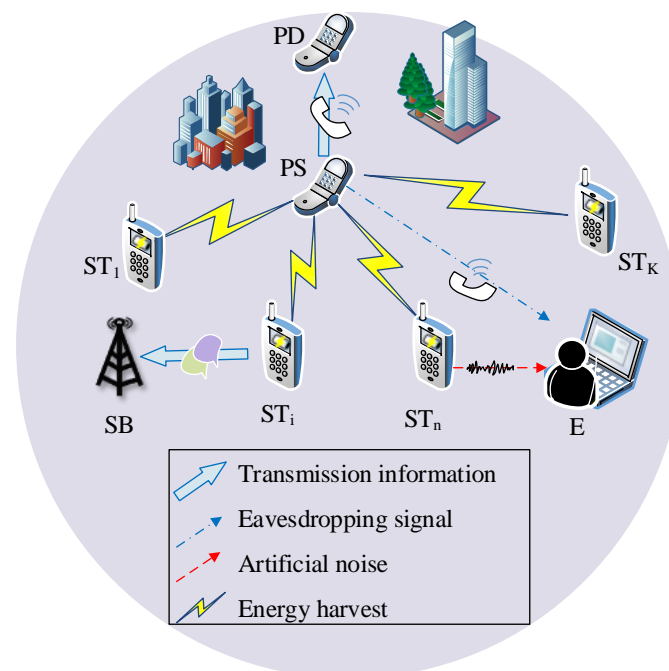
Meanwhile, the above-mentioned works focus on the secrecy performance of wireless communication without considering energy efficiency, which is a key problem in CIoT [22–25]. To enhance the energy efficiency, one of the most dominant methods is Energy Harvesting (EH), which harvests energy from the surroundings and prolongs the service life of wireless networks [26–28]. Furthermore, the performance of cognitive wireless networks with EH has been studied in recent years. For example, the secondary outage probability (OP) of EH cognitive radio systems was investigated in [29,30], where the opportunity relay selection (ORS) was used to select the best relay collaborative information transmission. In addition, some researchers are devoted to maximizing the throughput of EH cognitive radio networks, in which SUs collect energy from PUs. Specifically, Zheng et al. [31] considered three typical scenarios under the two cooperation modes of energy and joint mode to explore the factors affecting throughput. Furthermore, Liu et al. [32] analyzed the factors affecting the final decision threshold (k) and developed the optimal cooperative spectrum sensing (CSS) strategy according to the appropriate k value to maximize the throughput.

At present, EH combined with PLS has also attracted widespread attention [33–35]. Reference [33] adopted the relay protocol based on time switching, and EH technology is used to assist the relay and jammer to transmit secret and jamming signals. The security outage probability of the system is studied through two relay and jammer selection schemes. Reference [34] investigated the PLS of energy-harvesting cognitive radio networks and compared the security–reliability tradeoff (SRT) performance of the channel-aware user scheduling (CaUS) and energy-aware user scheduling (EaUS) methods. Reference [35] further analyzed the SRT of an energy-harvesting cooperative cognitive radio system and proposed two relay selection schemes to improve the security of cognitive users. Table 1 is a summary of some related works. The above works were committed to using EH to enhance the power of SUs or relays so as to assist SUs in transmitting data. Nonetheless, how to use energy harvesting to raise the confidentiality performance of PUs remains an open problem in FL over CIoT.

To improve the confidentiality performance of PUs, we integrate the advantages of the PLS technology and EH method into CIoT, which consists of multiple secondary transmitters (STs). The system scenario is shown in Figure 1. Meanwhile, we propose an ST transmission protocol by using cooperative transmission and friendly jamming. In the proposed protocol, STs obtain energy from the primary source (PS) in the first stage of the transmission slot and then transmit the signal in the second stage of the transmission slot to improve energy efficiency and spectrum utilization. In other words, a secondary transmitter (ST), which meets the interference threshold and can offer the best information transmission for SUs, is first chosen to share the PUs' spectrum. Another ST, which meets the interference threshold and offers the optimal security performance for PUs, is then chosen to transmit AN. To invigorate ST as the friendly jammer, the interference threshold for SUs is relaxed by the PUs.

Table 1. Summary of some related works.

Methods	Major Domain	Metrics	Technique	Main Contributions
[15]	PLS	perfect secrecy capacity	algebraic Riccati equation	The perfect secrecy capacity of multi antenna MIMO channel is calculated.
[21]	PLS	secrecy outage probability	friendly jammer, AN	Legitimate users achieved better secrecy performance.
[32]	PLS, CR	throughput	CSS	According to the appropriate K value, an optimal CSS strategy is developed to maximize throughput.
[33]	PLS, EH, CR	secrecy outage probability (SOP)	relay, jammer	It deduced the exact and asymptotic expressions of SOP.
[34]	PLS, EH, CR	OP, IP	SRT	The results revealed that there is a constraint relationship between reliability and safety.
[35]	PLS, EH, CR	OP, IP	SRT	It proposed two user-scheduling methods to improve the performance of secondary users.
Ours	PLS, EH, CR	OP, IP	dual secondary transmitter selection, AN	It improved the security performance of primary users and the transmission performance of secondary users.

**Figure 1.** System scenario.

The mainly contributions of this paper are summarized as follows:

- We propose a secrecy transmission protocol based on Energy Harvesting (EH) and jammer selection to improve the PLS of PUs for FL, where the AN is transmitted by a cooperative jammer to obstruct eavesdroppers. Moreover, the influence of the basic power of the secondary transmitter on EH and the primary users is considered. In addition, the secondary outage performance is enhanced due to cooperation compensation and multi-user diversity gain.
- A dual secondary transmitter selection scheme is proposed to determine the secondary signal transmitter and friendly jammer. The ST that can offer the smallest OP is

selected to transmit model parameters. Thus, the secondary transmission performance is enhanced by the ST selection. Another ST that can provide the smallest intercept probability (IP) is selected to transmit AN. Therefore, the primary security performance is enhanced by the friendly jammer selection.

- To compare the proposed protocol with optimal secondary transmission selection (OSTS) protocol, we derived the closed-form expressions of OP and IP of PUs and OP of SUs over Rayleigh fading channel for the above two protocols, respectively.
- The simulation results show that our protocol achieves better security performance than the OSTS and Optimal Cooperative Jammer Selection (OCJS) methods. Moreover, the secondary outage probabilities of the proposed scheme are lower than the OSTS and OCJS in high primary SNR, respectively. Furthermore, we improve the confidentiality of PUs and explore the influence of different parameters on the security performance.

The remainder of the paper is summarized as follows. An Energy-Harvesting Cognitive underlay system model and OSTS model is presented in Section 2. Section 3 presents OP and IP analysis for the cooperation transmission protocol. The OP and IP are analyzed for the OSTS model in Section 4. The numerical results of the performance comparison between the two methods are shown in Section 5. Finally, Section 6 contains the summary.

Notations: $|h_P|^2$, $|h_{PE}|^2$, $|h_{PS_n}|^2$, $|h_{S_nE}|^2$, $|h_{S_iE}|^2$, $|h_{PS_i}|^2$, $|h_{S_iD}|^2$, $|h_{S_i}|^2$, and $|h_{PB}|^2$ mean the channel coefficients from PS→PD, PS→E, PS→ST_n, ST_n→E, ST_i→E, PS→ST_i, ST_i→PD, ST_i→SB, and PS→SB, respectively. All channels in this paper are considered to experience quasi-static Rayleigh fading, and the channel gain coefficient $|h_v|^2$ is regarded as an independently exponentially distributed random variable with a mean of σ_v^2 . Namely, the Probability Density Function (PDF) of $|h_v|^2$ is expressed as follows:

$$f_{|h_v|^2}(x) = \frac{1}{\sigma_v^2} \exp\left(-\frac{x}{\sigma_v^2}\right), \quad (1)$$

where $v \in \{PE, PS_n, S_nE, S_iE, PS_i, S_iD, S_i, PB\}$. R_P and R_S mean the minimum data rates of PUs and SUs, respectively. P_P and P_{S_i} represent the transmit powers of PS and ST_i, respectively. We assume that the received noises of all receivers are zero-mean Additive White Gaussian Noises (AWGNs) with a variance of N_0 . $\Pr\{X\}$ and $E[X]$ mean the probability and expected value of an event X .

2. System Model Descriptions

2.1. The Energy-Harvesting Cognitive Underlay System Model

We consider an Energy-Harvesting Cognitive underlay system model, which is comprised of a primary pair (PS-PD), an eavesdropper (E), a secondary base station (SB) and K secondary transmitters (ST_{*i*}, where $i \in \mathcal{O} = \{1, 2, \dots, K\}$). The model is shown in Figure 2. In this model, secondary users can simultaneously access the licensed band with the primary system as long as the QoS of primary user is able to guarantee. Because of the battery-limited nature of ST_{*i*}, the EH technology is utilized to extend the network lifetime. The eavesdropper is very interested in the primary information. Thus, it tries to overhear and tap the active transmissions of the PS all the time. Moreover, the model can be applied to device-to-device (D2D) communication scenarios, and D2D users equipped with energy harvesters can play as the friendly jammers.

In the proposed protocol, one secondary transmitter denoted by ST_{*i*}, which can provide the best secondary outage performance, is selected to deliver secondary signals. Another secondary transmitter denoted by ST_{*n*}, which can provided the best primary intercept performance, is selected to transmit AN, where $i, n \in \mathcal{O}$ and $i \neq n$. The AN is produced by pseudo-random sequences known to PD and SB but unknown to E. Thus, AN makes no difference to PD and SB but causes serious influence to E. The signal transmission power at ST_{*i*} is determined by the combination of the harvesting energy, initial energy, and interference threshold. For the selfishness of ST, however, the signal transmission power at

ST_n is just determined by the harvesting energy. The detailed transmission mechanism and secondary transmitter selection scheme are introduced in the next subsection.

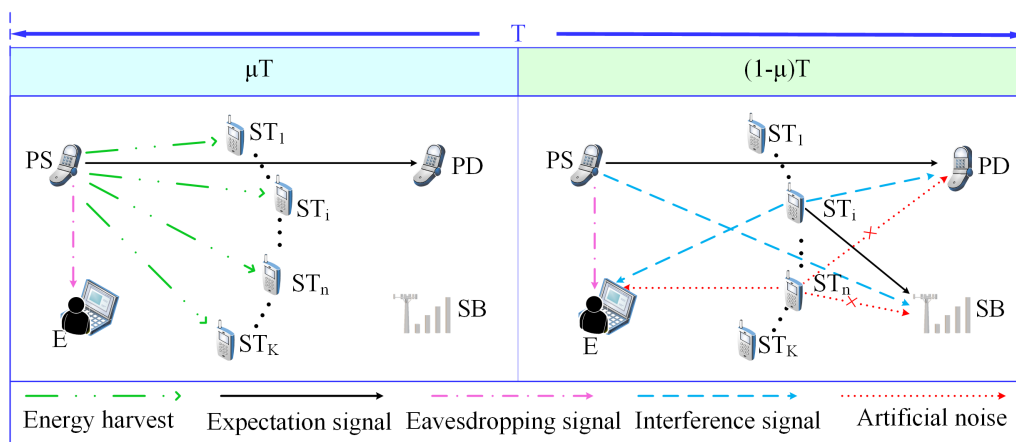


Figure 2. An energy-harvesting cognitive underlay system model. (μT : the segment slot for energy harvest and only primary signal transmission. $(1 - \mu)T$: the segment slot for primary and secondary signals transmission.)

2.2. Information Transmission

In this paper, the message transmission mechanism of the primary system is the same as that in traditional underlay cognitive networks, i.e., the primary data are continuously transmitted over the entire time slot. Moreover, the time slot receiver protocol for EH and information transmission at ST_i is employed, which is also used in [36]. Specifically, the total communication time slot consists of two segments: ST_i collects energy from PS in the front segment denoted as μT and transmits secondary information or artificial noise in the back segment denoted as $(1 - \mu)T$, where $0 \leq \mu \leq 1$ represents the slot split ratio and T represents the total length of each time slot. According to [37], the gathering energy at ST_i in the front segment slot can be presented as follows:

$$E_{ST_i} = \eta \mu T P_P |h_{PS_i}|^2, \tag{2}$$

where $0 \leq \eta \leq 1$ means the energy transfer efficiency. Meanwhile, a collection of working secondary transmitters that meet the interference threshold is expressed as Q [38]. When $Q = \emptyset$, only PS transmits the signals; the secondary transmission is interrupted. Thus, the received signals at PD and E are expressed as in (3) and (4), respectively. The instantaneous capacities of the PS→PD link and the PS→E link are expressed as in (5) and (6), respectively.

$$r_{P1}(t) = \sqrt{P_P} h_P x_P(t) + n_P(t), \tag{3}$$

$$r_{E1}(t) = \sqrt{P_P} h_{PE} x_P(t) + n_E(t), \tag{4}$$

$$C_{P1} = \mu T \log_2 \left(1 + \frac{P_P |h_P|^2}{N_0} \right), \tag{5}$$

$$C_{E1} = \mu T \log_2 \left(1 + \frac{P_P |h_{PE}|^2}{N_0} \right). \tag{6}$$

It assumes that the initial energy owned by ST_i can be expressed as $E_0 = P_0 T$, where P_0 is the basic transmission power. On the one hand, the transmitted power at ST_i in the $(1 - \mu)T$ segment slot depends on the combination of the harvesting energy and initial

energy. On the other hand, the interference to PD caused by ST_i must be lower than the maximum tolerable interference level that is denoted by I in the underlay cognitive model. Thus, the transmitted power at ST_i in the $(1 - \mu)T$ segment slot can be expressed as

$$P_{S_i} = \min \left(\frac{I}{|h_{S_i,D}|^2}, \frac{\eta\mu P_P |h_{PS_i}|^2 + P_0}{1 - \mu} \right). \quad (7)$$

When $Q \neq \emptyset$, PS transmits the primary signals. Meanwhile, in the back segment slot, secondary signals are transmitted by ST_i to SB and an artificial noise is delivered by ST_n . Therefore, the received signals at PD, SB, and E are expressed as

$$r_{P2}(t) = \sqrt{P_P} h_P x_P(t) + \sqrt{P_{S_i}} h_{S_i,D} x_S(t) + n_P(t), \quad (8)$$

$$r_{S_i}(t) = \sqrt{P_{S_i}} h_{S_i} x_S(t) + \sqrt{P_P} h_{PB} x_P(t) + n_{S_i}(t), \quad (9)$$

$$r_{E2}(t) = \sqrt{P_P} h_{PE} x_P(t) + \sqrt{P_{S_n}} h_{S_n,E} x_n(t) + \sqrt{P_{S_i}} h_{S_i,E} x_S(t) + n_E(t), \quad (10)$$

where P_{S_n} is the transmitted power at ST_n . Because the energy at ST_n is limited and the AN makes no difference to PD, P_{S_n} can be set to $\eta\mu P_P |h_{PS_n}|^2 / (1 - \mu)$. $x_n(t)$, $x_P(t)$, and $x_S(t)$ indicate the AN, the PUs' message symbol, and the SUs' message symbol, respectively. Moreover, $n_P(t)$, $n_S(t)$, and $n_E(t)$ indicate noises at PD, SB, and E, respectively. Moreover, $E[|x_\alpha(t)|^2] = 1$, where $\alpha \in \{P, S, n\}$. According to the above conditions, the instantaneous capacities of the PS \rightarrow PD link, the $ST_i \rightarrow$ SB link, and the PS \rightarrow E link transmission can be obtained by (11)–(13), respectively.

$$C_{P2} = (1 - \mu) T \log_2 \left(1 + \frac{P_P |h_P|^2}{P_{S_i} |h_{S_i,D}|^2 + N_0} \right), \quad (11)$$

$$C_{S_i} = (1 - \mu) T \log_2 \left(1 + \frac{P_{S_i} |h_{S_i}|^2}{P_P |h_{PB}|^2 + N_0} \right), \quad (12)$$

$$C_{E2} = (1 - \mu) T \log_2 \left(1 + \frac{P_P |h_{PE}|^2}{P_{S_n} |h_{S_n,E}|^2 + P_{S_i} |h_{S_i,E}|^2 + N_0} \right). \quad (13)$$

During the back segment slot, the optimal secondary signal transmitter ST_{i^*} and the optimal friendly jammer ST_{n^*} are selected due to the multi-user scheduling scheme. For optimal secondary reliable transmission performance, the optimal secondary signal transmitter ST_{i^*} can be selected via the $ST_i \rightarrow$ SB link, i.e.,

$$i^* = \arg \max_{i^* \in O} (|h_{S_i}|^2). \quad (14)$$

Because the dual secondary transmitter selection is used, the optimal secondary signal transmitter cannot be played as the optimal friendly jammer, then $i, n \in O$ and $i \neq n$. For optimal primary security performance, the optimal friendly jammer ST_{n^*} can be selected via the $ST_n \rightarrow$ E link, i.e.,

$$n^* = \arg \max_{n^* \in O, n^* \neq i^*} (|h_{S_n,E}|^2). \quad (15)$$

2.3. The Optimal Secondary Transmission Selection Model

For comparison, we take the OSTs cognitive underlay model in [38] as the benchmark and further consider the battery-limited condition. The OSTs model consists of a primary pair (PS-PD), an eavesdropper (E), a secondary base station (SB) and K secondary trans-

mitters ($ST_i, i = 1, \dots, K$). The protocol also utilizes the friendly jamming technology to transmit AN and secondary signals by selecting an ST. There, the interference threshold for SUs is relaxed. Specifically, to linearly combine the AN with the secondary signal, the transmission power of ST_i is divided into ξ and $1 - \xi$, where $0 \leq \xi \leq 1$ means the power distribution factor. Then, the combined signal can be expressed as $\sqrt{1-\xi}x_n(t) + \sqrt{\xi}x_S(t)$. Furthermore, the energy-harvesting technology is not considered in the model, while security–reliability trade-off can be employed according to [34]. Since the interference caused by ST_i must be lower than a threshold settled by the primary system in cognitive underlay models, the transmitted power at ST_i is limited to P_0 for the battery-limited condition; then, the transmitted power at ST_i can be expressed as

$$P_{S_i}^{OSTS} = \min\left(I/|h_{S_iD}|^2, P_0\right). \quad (16)$$

When only PS transmits the signals, the STs do not work (namely, $Q^{OSTS} = \emptyset$). The signals at PD and E are like (3) and (4), respectively. The instantaneous capacities of the PS→PD link and the PS→E link transmission can be expressed as in (17) and (18), respectively.

$$C_{P1}^{OSTS} = \log_2\left(1 + \frac{P_P|h_P|^2}{N_0}\right), \quad (17)$$

$$C_{E1}^{OSTS} = \log_2\left(1 + \frac{P_P|h_{PE}|^2}{N_0}\right). \quad (18)$$

When $Q^{OSTS} \neq \emptyset$, the secondary signal and primary signal coexist in the licensed spectrum in the OSTS model. The received signals at PD, SB, and E are expressed as (19)–(21), respectively.

$$r_{P2}^{OSTS}(t) = \sqrt{P_P}h_P x_P(t) + \sqrt{\xi P_{S_i}^{OSTS}}h_{S_iD}x_S(t) + n_P(t), \quad (19)$$

$$r_{S_i}^{OSTS}(t) = \sqrt{\xi P_{S_i}^{OSTS}}h_{S_i}x_S(t) + \sqrt{P_P}h_{PB}x_P(t) + n_{S_i}(t), \quad (20)$$

$$r_{E2}^{OSTS}(t) = \sqrt{P_P}h_{PE}x_P(t) + \left[\sqrt{(1-\xi)P_{S_i}^{OSTS}}x_n(t) + \sqrt{\xi P_{S_i}^{OSTS}}x_S(t)\right]h_{S_iE} + n_E(t). \quad (21)$$

Thus, the instantaneous capacities of the PS→PD link, the ST_i →SB link, and the PS→E link transmission can be written as (22)–(24), respectively.

$$C_{P2}^{OSTS} = \log_2\left[1 + \frac{P_P|h_P|^2}{\xi P_{S_i}^{OSTS}|h_{S_iD}|^2 + N_0}\right], \quad (22)$$

$$C_S^{OSTS} = \log_2\left[1 + \frac{\xi P_{S_i}^{OSTS}|h_{S_i}|^2}{P_P|h_{PB}|^2 + N_0}\right], \quad (23)$$

$$C_E^{OSTS} = \log_2\left[1 + \frac{P_P|h_{PE}|^2}{P_{S_i}^{OSTS}|h_{S_iE}|^2 + N_0}\right]. \quad (24)$$

As is well known, multi-user diversity technology can effectively improve the performance of communication systems. Similar to [36], a security–reliability trade-off can be used to enhance the security performance of the OSTS model. Furthermore, the selection

criteria for ST_{i^*} , which may share PUs' spectrum for transmitting secondary signals, can be shown as

$$ST_{i^*} = \arg \min_{i^* \in \mathcal{O}} \Pr \left\{ C_S^{OSTS} < R_S \right\} = \arg \max_{i^* \in \mathcal{O}} \left(|h_{S_i E}|^2 \right). \quad (25)$$

3. The OP and IP Analysis for the Cooperation Transmission and Energy-Harvesting Protocol

As described in [39,40], OP and IP are two vital parameters to judge the reliability and secrecy of information transmission in communication. Therefore, we analyze these two parameters in detail.

3.1. The Primary OP Analysis

As described in [38], when $Q \neq \emptyset$, we denote $Q = Q_l$. In that case, both PS and ST_i transmit signals, where $ST_i \in Q_l$ and $l=1, 2, \dots, 2^K - 1$. The amount of elements in the collection Q_l is L . $Q_l = \{ST_i | C_{P2} \geq R_P, i \in \{1, \dots, K\}\}$ and $\bar{Q}_l = \{ST_i | C_{P2} < R_P, i \in \{1, \dots, K\}\}$. $Q_l \cup \bar{Q}_l = \{ST_1, ST_2, \dots, ST_K\}$. Ψ_P is defined as the transmission outage event of a primary system. We know that the event Ψ_P is considered to happen when $C_{P2} < R_P$. The OP of PUs can be given by

$$P_{out} = \Pr\{Q = \emptyset\} \Pr\{\Psi_P | Q = \emptyset\} + \sum_{l=1}^{2^K-1} \Pr\{Q = Q_l\} \Pr\{\Psi_P | Q = Q_l\}. \quad (26)$$

After that, $\Pr\{Q = \emptyset\}$ can be shown as

$$\begin{aligned} \Pr\{Q = \emptyset\} &= \prod_{i=1}^K \Pr\{C_{P2} < R_P\} \\ &= \prod_{i=1}^K \Pr \left\{ (1 - \mu) T \log_2 \left(1 + \frac{P_P |h_P|^2}{P_{S_i} |h_{S_i D}|^2 + N_0} \right) < R_P \right\} \\ &= \prod_{i=1}^K \Pr \left\{ \frac{P_P |h_P|^2}{P_{S_i} |h_{S_i D}|^2 + N_0} < 2^{\frac{R_P}{(1-\mu)T}} - 1 \right\}, \end{aligned} \quad (27)$$

where C_{P2} is given by (11). According to the results given by (A1)–(A3) in Appendix A, the final expression of $\Pr\{Q = \emptyset\}$ is

$$\Pr\{Q = \emptyset\} = \prod_{i=1}^K \Pr\{\text{Ch1} \times \text{Ch2}\} \quad (28)$$

Moreover, $\Pr\{\Psi_P | Q = \emptyset\}$ and $\Pr\{Q = Q_l\}$ can be calculated by (29) and (30), respectively.

$$\begin{aligned} \Pr\{\Psi_P | Q = \emptyset\} &= \Pr \left\{ \mu T \log_2 \left(1 + \frac{P_P |h_P|^2}{N_0} \right) < R_P \right\} \\ &= 1 - \exp \left(- \frac{N_0 \left[2^{R_P / (\mu T)} - 1 \right]}{P_P \sigma_P^2} \right), \end{aligned} \quad (29)$$

$$\begin{aligned} \Pr\{Q = Q_l\} &= \prod_{i \in \bar{Q}_l} \Pr\{C_{P2} < R_P\} \prod_{j \in Q_l} \Pr\{C_{P2} \geq R_P\} \\ &= \prod_{i \in \bar{Q}_l} (\text{Ch1} \times \text{Ch2}) \prod_{j \in Q_l} (1 - \text{Ch1} \times \text{Ch2}). \end{aligned} \quad (30)$$

According to the definition of the collection Q_l , we can know that $\Pr\{\Psi_P | Q = Q_l\} = 0$. Thus, the OP of PUs is derived by substituting (28)–(30) and substituting $\Pr\{\Psi_P | Q = Q_l\} = 0$ into (26). Here, Ch 1 and Ch 2 are calculated by (A2) and (A3), respectively.

3.2. The Secondary OP Analysis Based on Optimal Selection Strategy

As described in [38], Ψ_S is defined as the transmission outage event of a secondary system. The event Ψ_S is indicated to happen when $C_{S_i} < R_P$. In addition, the event Ψ_S will happen when all STs do not work, i.e., $Q = \emptyset$ or the QoS of secondary users is not satisfied ($Q \neq \emptyset$). In the proposed protocol based on an optimal selection strategy, an optimal ST_i is selected to transmit the secondary information, which can provide the best secondary transmission performance. The secondary outage probability of the proposed protocol based on optimal selection strategy can be written as

$$S_{out}^{opt} = \Pr\{Q = \emptyset\} \Pr\{\Psi_S|Q = \emptyset\} + \sum_{l=1}^{2^K-1} \Pr\{Q = Q_l\} \Pr\{\Psi_S|Q = Q_l\}. \quad (31)$$

Furthermore, $\Pr\{\Psi_S|Q = Q_l\}$ can be calculated as

$$\begin{aligned} & \Pr\{\Psi_S|Q = Q_l\} \\ &= \Pr\left\{(1-\mu)T \log_2\left(1 + \frac{P_{S_i} \max(|h_{S_i}|^2)}{P_P|h_{PB}|^2 + N_0}\right) < R_S\right\} \\ &= \prod_{i=1}^L \Pr\left\{\frac{P_{S_i}|h_{S_i}|^2}{P_P|h_{PB}|^2 + N_0} < 2^{\frac{R_S}{(1-\mu)T}} - 1\right\}. \end{aligned} \quad (32)$$

According to the results given by (A4)–(A6) in Appendix A, the final expression of $\Pr\{\Psi_S|Q = Q_l\}$ is

$$\Pr\{\Psi_S|Q = Q_l\} = \prod_{i=1}^K \Pr\{1 - \text{Ch3} \times \text{Ch4}\} \quad (33)$$

We know that $\Pr\{\Psi_S|Q = \emptyset\} = 1$. The OP of SUs in our protocol based on the optimal selection strategy for ST_{i^*} can be obtained by substituting (28)–(33), and $\Pr\{\Psi_S|Q = \emptyset\} = 1$ into (31). Here, Ch 1–Ch 4 are calculated by (A2)–(A6), respectively.

3.3. The Primary IP Analysis Based on Optimal Selection Strategy

According to [38], Ψ_{int} denotes the transmission intercept event of PUs. Furthermore, Ψ_{int} is implied to occur when $R_P < C_{E2}$. When $Q \neq \emptyset$, the event Ψ_{int} may happen. Since $i, n \in \mathcal{O}$ and $i \neq n$, the number of secondary transmitters selected at this condition is $K - 1$. Let $M = K - 1$, where $Q_l \cup \overline{Q_l} = \{ST_1, ST_2, \dots, ST_M\}$. Hence, the primary intercept probability of the proposed protocol based on the optimal selection strategy can be written as

$$P_{int}^{opt} = \Pr\{Q = \emptyset\} \Pr\{\Psi_{int}|Q = \emptyset\} + \sum_{l=1}^{2^M-1} \Pr\{Q = Q_l\} \Pr\{\Psi_{int}|Q = Q_l\}. \quad (34)$$

Next, $\Pr\{\Psi_{int}|Q = \emptyset\}$ can be shown as

$$\begin{aligned} \Pr\{\Psi_{int}|Q = \emptyset\} &= \Pr\{C_{E1} \geq R_P\} = \Pr\left\{\mu T \log_2\left(1 + \frac{P_P|h_{PE}|^2}{N_0}\right) \geq R_P\right\} \\ &= \Pr\left\{\frac{P_P|h_{PE}|^2}{N_0} \geq 2^{\frac{R_P}{\mu T}} - 1\right\} = \exp\left(-\frac{N_0 \left[2^{\frac{R_P}{\mu T}} - 1\right]}{P_P \sigma_{PE}^2}\right). \end{aligned} \quad (35)$$

As described in (15), ST_{n^*} , which has the best channel state conditions to E, is selected to transmit artificial noises to interfere with eavesdropping. Thus, $\Pr\{\Psi_{int}|Q = Q_l\}$ can be derived as

$$\begin{aligned}
& \Pr\{\Psi_{\text{int}}|Q = Q_l\} \\
&= \Pr\{C_{E2} \geq R_P\} = \Pr\left\{\frac{P_P|h_{PE}|^2}{P_{S_{n^*}}|h_{S_{n^*}E}|^2 + P_{S_i}|h_{S_iE}|^2 + N_0} \geq 2^{\frac{R_P}{(1-\mu)T}} - 1\right\} \\
&= \prod_{n=1}^L \Pr\left\{\frac{P_P|h_{PE}|^2}{P_{S_n}|h_{S_nE}|^2 + P_{S_i}|h_{S_iE}|^2 + N_0} \geq \Delta_P\right\} \\
&= \prod_{n=1}^L \Pr\left\{\frac{P_{S_n}|h_{S_nE}|^2 + P_{S_i}|h_{S_iE}|^2 + N_0}{P_P|h_{PE}|^2} \leq \frac{1}{\Delta_P}\right\} \\
&= \prod_{n=1}^L \left(1 - \Pr\left\{\min\left(\frac{I}{|h_{S_iD}|^2}, \frac{\eta\mu P_P|h_{PS_n}|^2 + P_0}{1-\mu}\right)|h_{S_iE}|^2 + \frac{\eta\mu P_P|h_{PS_n}|^2|h_{S_nE}|^2}{1-\mu} + N_0\right.\right. \\
&\quad \left.\left. > \frac{P_P|h_{PE}|^2}{\Delta_P}\right\}\right) \\
&= \prod_{n=1}^L \left[1 - \Pr\left\{\underbrace{\frac{I|h_{S_iE}|^2}{|h_{S_iD}|^2} + \frac{\eta\mu P_P|h_{PS_n}|^2|h_{S_nE}|^2}{1-\mu} + N_0}_{\text{Ch5}} > \frac{P_P|h_{PE}|^2}{\Delta_P}\right\}\right. \\
&\quad \left.\times \Pr\left\{\underbrace{\frac{(\eta\mu P_P|h_{PS_i}|^2 + P_0)|h_{S_iE}|^2 + \eta\mu P_P|h_{PS_n}|^2|h_{S_nE}|^2}{1-\mu} + N_0}_{\text{Ch6}} > \frac{P_P|h_{PE}|^2}{\Delta_P}\right\}\right].
\end{aligned} \tag{36}$$

To sum up, the IP of PUs based on the optimal selection strategy for ST_{n^*} can be obtained by substituting (28), (30), (35), and (36) into (34), where Ch 1, Ch 2, Ch 5, and Ch 6 are calculated by (A2), (A3), (A7), and (A8), respectively.

4. The OP and IP Analysis for the Battery-Limited OSTS Protocol

In the battery-limited OSTS protocol, the security–reliability trade-off is presented to enhance the primary security performance. Specifically, ST_{i^*} , which has the best channel state conditions to SB, is selected for transmitting secondary data. Similar to the probability analysis of the proposed protocol, the OP of PUs and SUs, the IP of PUs are calculated by (37)–(39), respectively.

$$\begin{aligned}
P_{out}^{OSTS} &= \Pr\{Q^{OSTS} = \emptyset\} \Pr\{\Psi_P|Q^{OSTS} = \emptyset\} \\
&\quad + \sum_{l=1}^{2^K-1} \Pr\{Q^{OSTS} = Q_l\} \Pr\{\Psi_P|Q^{OSTS} = Q_l\},
\end{aligned} \tag{37}$$

$$\begin{aligned}
S_{out}^{OSTS} &= \Pr\{Q^{OSTS} = \emptyset\} \Pr\{\Psi_S|Q^{OSTS} = \emptyset\} \\
&\quad + \sum_{l=1}^{2^K-1} \Pr\{Q^{OSTS} = Q_l\} \Pr\{\Psi_S|Q^{OSTS} = Q_l\},
\end{aligned} \tag{38}$$

$$P_{\text{int}}^{\text{OSTS}} = \Pr\{Q^{\text{OSTS}} = \emptyset\} \Pr\{\Psi_{\text{int}}|Q^{\text{OSTS}} = \emptyset\} + \sum_{l=1}^{2^K-1} \Pr\{Q^{\text{OSTS}} = Q_l\} \Pr\{\Psi_{\text{int}}|Q^{\text{OSTS}} = Q_l\}, \quad (39)$$

where $\Pr\{\Psi_S|Q^{\text{OSTS}} = \emptyset\} = 1$, $\Pr\{\Psi_P|Q^{\text{OSTS}} = Q_l\} = 0$, and the rest of the probabilities in (37)–(39) are expressed by (40)–(46), respectively.

$$\Pr\{\Psi_P|Q^{\text{OSTS}} = \emptyset\} = \Pr\left\{\log_2\left(1 + \frac{P_P|h_P|^2}{N_0}\right) < R_P\right\} = 1 - \exp\left(-\frac{N_0\rho_P}{P_P\sigma_P^2}\right), \quad (40)$$

$$\begin{aligned} \Pr\{Q^{\text{OSTS}} = \emptyset\} &= \prod_{i=1}^K \Pr\{C_{P2}^{\text{OSTS}} < R_P\} \\ &= \prod_{i=1}^K \Pr\left\{\log_2\left(1 + \frac{P_P|h_P|^2}{\xi P_{S_i}^{\text{OSTS}}|h_{S_iD}|^2 + N_0}\right) < R_P\right\} \\ &= \prod_{i=1}^K \Pr\left\{\frac{P_P|h_P|^2}{\xi P_{S_i}^{\text{OSTS}}|h_{S_iD}|^2 + N_0} < 2^{R_P} - 1\right\}, \end{aligned} \quad (41)$$

where $\rho_P = 2^{R_P} - 1$ and C_{P2}^{OSTS} are given by (22). According to the results given by (A9)–(A11) in Appendix A, the final expression of $\Pr\{Q^{\text{OSTS}} = \emptyset\}$ is

$$\Pr\{Q^{\text{OSTS}} = \emptyset\} = \prod_{i=1}^K \Pr\{\text{Ch7} \times \text{Ch8}\} \quad (42)$$

According to (41) and (42), we have

$$\begin{aligned} \Pr\{Q^{\text{OSTS}} = Q_l\} &= \prod_{i \in \overline{Q_l}} \Pr\{C_{P2}^{\text{OSTS}} < R_P\} \prod_{j \in Q_l} \Pr\{C_{P2}^{\text{OSTS}} \geq R_P\} \\ &= \prod_{i \in \overline{Q_l}} (\text{Ch7} \times \text{Ch8}) \prod_{j \in Q_l} (1 - \text{Ch7} \times \text{Ch8}). \end{aligned} \quad (43)$$

In addition, $\Pr\{\Psi_S|Q^{\text{OSTS}} = Q_l\}$ can be written as follows:

$$\begin{aligned} \Pr\{\Psi_S|Q^{\text{OSTS}} = Q_l\} &= \arg \min_{i^* \in \mathcal{O}} \Pr\{C_S^{\text{OSTS}} < R_S\} \\ &= \Pr\left\{\frac{\xi P_{S_i}^{\text{OSTS}} \max_{i^* \in \mathcal{O}}(|h_{S_iE}|^2)}{P_P|h_{PB}|^2 + N_0} < 2^{R_S} - 1\right\} \\ &= \prod_{i=1}^L \Pr\left\{\frac{\xi P_{S_i}^{\text{OSTS}}|h_{S_iE}|^2}{P_P|h_{PB}|^2 + N_0} < 2^{R_S} - 1\right\} \\ &= \prod_{i=1}^L \left[1 - \Pr\left\{\min(I/|h_{S_iD}|^2, P_0) \cdot \xi|h_{S_i}|^2 > \rho_S(P_P|h_{PB}|^2 + N_0)\right\}\right] \\ &= \prod_{i=1}^L \left[1 - \underbrace{\Pr\left\{\frac{\xi I|h_{S_i}|^2/|h_{S_iD}|^2}{P_P|h_{PB}|^2 + N_0} > \rho_S\right\}}_{\text{Ch9}} \cdot \underbrace{\Pr\left\{\frac{\xi P_0|h_{S_i}|^2}{P_P|h_{PB}|^2 + N_0} > \rho_S\right\}}_{\text{Ch10}}\right], \end{aligned} \quad (44)$$

where $\rho_S = 2^{R_S} - 1$. Considering $Y_1 = |h_{S_i}|^2 / |h_{S_i,D}|^2$ and using the PDF of Y_1 , which is calculated in Appendix B, Ch9 and Ch10 can be derived as (A12) and (A13), respectively.

Furthermore, $\Pr\{\Psi_{\text{int}}|Q^{OSTS} = \emptyset\}$ can be derived as

$$\Pr\{\Psi_{\text{int}}|Q^{OSTS} = \emptyset\} = \Pr\left\{X_6 \geq \frac{N_0(2^{R_P} - 1)}{P_P}\right\} = e^{-\frac{N_0\rho_P}{P_P\sigma_{P_E}^2}}. \quad (45)$$

Following (25), the $\Pr\{\Psi_{\text{int}}|Q^{OSTS} = Q_I\}$ can be written as (46), while Ch11 and Ch12 can be derived as (A14) and (A15), respectively.

$$\begin{aligned} \Pr\{\Psi_{\text{int}}|Q^{OSTS} = Q_I\} &= \Pr\{C_E^{OSTS} \geq R_P\} \\ &= \Pr\left\{\frac{P_P|h_{P_E}|^2}{P_{S_i}^{OSTS}|h_{S_i,E}|^2 + N_0} \geq 2^{R_P} - 1\right\} \\ &= 1 - \Pr\{P_P|h_{P_E}|^2 < \rho_P(P_{S_i}^{OSTS}|h_{S_i,E}|^2 + N_0)\} \\ &= 1 - \Pr\{P_P|h_{P_E}|^2 < \rho_P(\min(I/|h_{S_i,D}|^2, P_0) \cdot |h_{S_i,E}|^2 + N_0)\} \\ &= 1 - \left[\underbrace{\Pr\{P_P|h_{P_E}|^2 < \rho_P(I|h_{S_i,E}|^2/|h_{S_i,D}|^2 + N_0)\}}_{\text{Ch11}} \right] \\ &\quad \times \left[\underbrace{\Pr\{P_P|h_{P_E}|^2 < \rho_P(P_0|h_{S_i,E}|^2 + N_0)\}}_{\text{Ch12}} \right]. \end{aligned} \quad (46)$$

5. Numerical Results

This section gives the simulation results of the comparison between the proposed protocol and the battery-limited OSTS and OCJS protocols [38]. We not only evaluate the confidentiality performance but also pay attention to the transmission performance. To repay the friendly jammer, PUs relax the interference threshold, which leads to reducing the R_P . Therefore, we set the rate of the PUs of the battery-limited OSTS, OCJS and the proposed model to $R_P = 0.5$ Bit/s/Hz. We assume that $R_S = 0.5$ Bit/s/Hz, $K = 3$, $\eta = 0.7$, $\mu = 0.5$, $T = 1$ s, $\xi = 0.5$, $I = P_P$ ($r_2 = 10 \log(I/N_0)$), $r_3 = 10 \log(P_0/N_0) = 5$ dB and the channel coefficients σ_P^2 , $\sigma_{S_D}^2$, $\sigma_{P_B}^2$, $\sigma_{P_E}^2$, $\sigma_{P_S}^2$, and $\sigma_{P_{S_n}}^2$ are normalized to 1, $\sigma_{S_n,E}^2 = 3$, $\sigma_{S_i,E}^2 = 1.5$ and $\sigma_{S_i}^2 = 4$ in our experiments.

Figure 3 displays the OPs of PUs or SUs versus r_1 ($r_1 = 10 \log(P_P/N_0)$) of the OSTS and OCJS models as well as the proposed model with different values of K . In order to analyze the gain caused by the increase of K value, we can set that $K = 3, 4$, and all transmission performances are ameliorated with the increase of K as a result of the multi-user diversity gain. The primary transmission performance improved with the increase of r_1 in the three models. This is because primary users can obtain more primary information in the high SNR. However, the OSTS and OCJS schemes can offer a lower outage probability than the proposed scheme. This is because the proposed scheme uses the EH technology of time allocation, which causes the instantaneous capacity of the PS \rightarrow PD link to become smaller and does not meet the minimum transmission rate of the primary system, resulting in transmission interruption. In addition, with the increase of SNR, the OPs of SUs of three models first decline and then raise. The declining trend is due to the increase of interference threshold ($r_2 = 10 \log(I/N_0)$) as the SNR of the primary network ($r_1 = 10 \log(P_P/N_0)$) increases, so that the power of the secondary transmitter increases and more information can be transmitted. In addition, the raising trend is because the interference at secondary users also increases when r_1 is too large. Furthermore, due to the EH technology, the power

of STs becomes larger, and the proposed scheme can achieve better secondary transmission performance under the condition of high SNR.

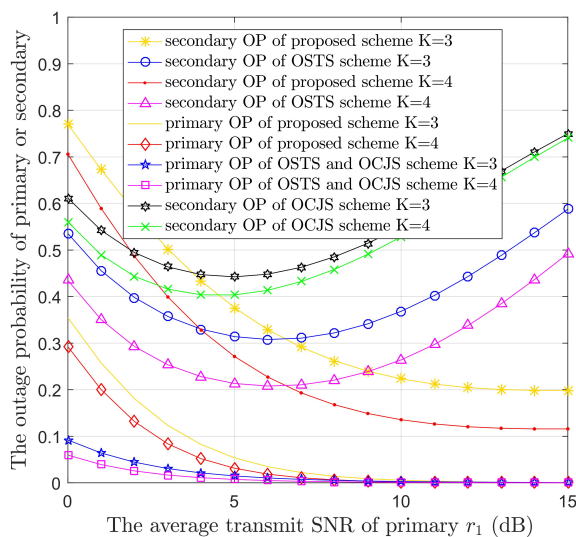


Figure 3. The OPs of PUs or SUs versus the average transmit SNR of primary (r_1) in the three protocols with different the number of STs (K).

Figure 4 displays the IPs of PUs versus r_1 in the three models with different values of K . The number of STs is 3 or 4. According to Figure 4, the PUs’ confidentiality performance is ameliorated in three models with the increase of the number of STs. The confidentiality performance of the proposed model is better than that of the battery-limited OSTS and OCJS models. In addition, the IPs of PUs decline with the raise of r_1 in the proposed model. This is because the ST_i can transmit AN to prevent eavesdropping and the ST_n has the best channel to E; then, ST_n can also increase interference with the eavesdropper. The short increasing trend is due to the lower power and poor performance of STs in the small value range of r_1 , and the interference to E is decreased. However, in the battery-limited OSTS and OCJS models, the confidentiality performance of the PUs increases as the r_1 increases. This is because the eavesdropper can obtain more primary information by a higher value of r_1 and ST_i has only a small part of power to transmit AN. This is the cause of the security performance deteriorating sharply. These phenomena are also shown in Figures 5–7.

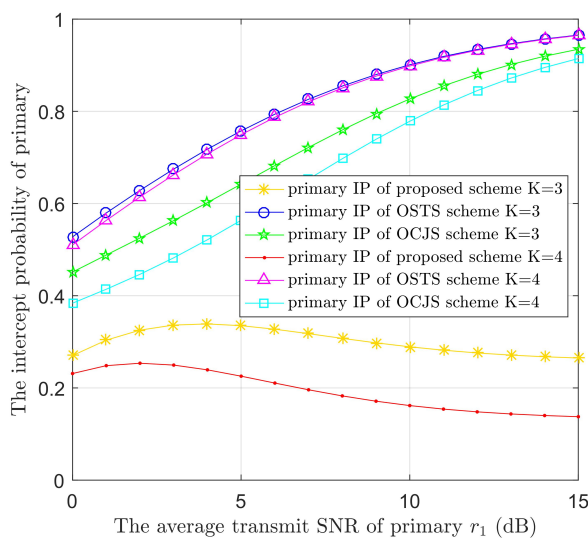


Figure 4. The IPs of the PUs versus the average transmit SNR of primary (r_1) in the three protocols with different numbers of STs (K).

Figure 5 illustrates the IPs of PUs versus r_1 in the three models with different $\sigma_{S_i,E}^2$. Since the interference channel gain of $\sigma_{S_i,E}^2$ is greater than the channel gain of $\sigma_{P,E}^2$ and smaller than the channel gain of $\sigma_{S_n,E}^2$, therefore, the channel coefficient $\sigma_{S_i,E}^2$ is equal to 1, 1.5 or 2. As described in Figure 5, the proposed model is able to offer better confidentiality performance in the same channel coefficient compared to [38]. Moreover, the confidentiality performance is ameliorated obviously in two models as the value of $\sigma_{S_i,E}^2$ becomes larger. This is because the $ST_i \rightarrow E$ link has better channel condition in a larger $\sigma_{S_i,E}^2$ value. In other words, the ST_i transmits more interference to the eavesdropper as the value of $\sigma_{S_i,E}^2$ increases. In the proposed model, both ST_n and ST_i interfere with the E. Nevertheless, the interference to E from ST_i is worse than that from ST_n . Hence, the PUs' secrecy performance is improved slightly. Moreover, the battery-limited OSTs and OCJS models interfere with E only from ST_i . However, the OCJS method selects the secondary transmitter that can provide the optimal intercept probability to E, so the security performance of OCJS is better than that of OSTs.

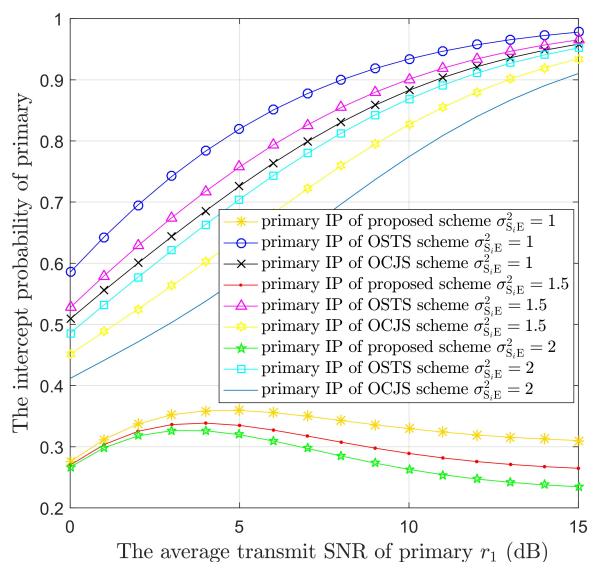


Figure 5. The IPs of the PUs versus the average transmit SNR of primary (r_1) in the three protocols with different channel coefficient ($\sigma_{S_i,E}^2$) values.

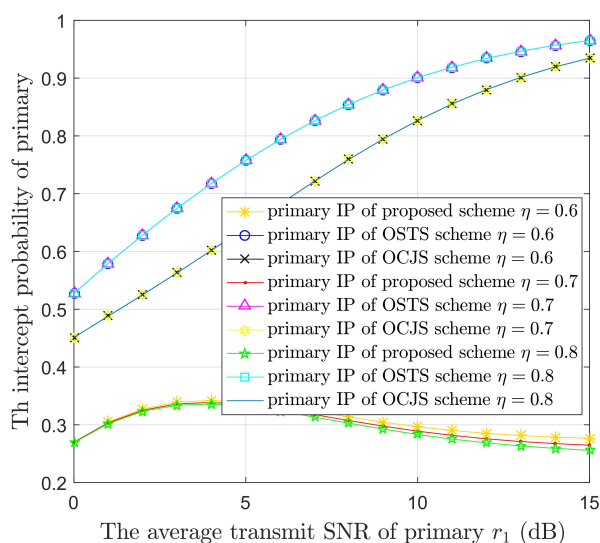


Figure 6. The IPs of the PUs versus the average transmit SNR of primary (r_1) in the three protocols with different energy transfer efficiency (η) values.

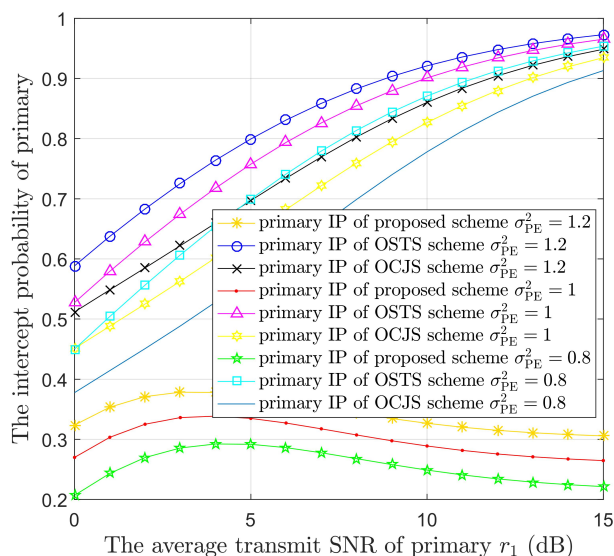


Figure 7. The IPs of the PUs versus the average transmit SNR of primary (r_1) in the three protocols with different channel coefficient (σ_{PE}^2) values.

Figure 6 illustrates the IPs of PUs versus r_1 in the three models with different η . The energy transfer efficiency η is equal to 0.6, 0.7 or 0.8, where the specific values set is referred to [30,41]. The confidentiality performance is ameliorated in the proposed model as η is raised. This is because the larger value of η means more energy can be used for the artificial noise transmission. Namely, STs transmit more interference to the eavesdropper as the value of η increases. Nonetheless, the primary security performance remains unchanged in the battery-limited OSTS and OCJS models. This is because energy harvesting is not considered in the OSTS and OCJS models. Then, the change of energy transfer efficiency η has no effect on the intercept probability.

Figure 7 illustrates the IPs of PUs versus r_1 in the three models with different values of σ_{PE}^2 . The channel coefficient σ_{PE}^2 equals to 1.2, 1 or 0.8. According to Figure 7, the confidentiality performance deteriorated with the increase of channel coefficient σ_{PE}^2 in the same model. This is because the PS→E link has better channel conditions in a larger σ_{PE}^2 value. In other words, the eavesdropper can obtain more primary information via a larger σ_{PE}^2 value. Furthermore, the proposed model also can provide the better primary confidentiality performance compared to [38].

6. Conclusions

The paper investigated the PLS of the underlying model of cognitive Internet of Things. We proposed an ST cooperative jammer selection transmission and energy-harvesting protocol to safeguard PUs and prevent eavesdropping. We also conducted a detailed theoretical study on the performance for the proposed protocol and the battery-limited OSTS protocol. The closed-form expressions of OP and IP of the above two models in Rayleigh fading channels were derived. Moreover, we also considered the OCJS model for further comparison in the experimental part. The final numerical results illustrate that the proposed protocol has better secrecy performance than the battery-limited OSTS and OCJS models due to ST selection transmission and energy harvesting. In addition, the proposed scheme achieves better secondary transmission performance under the condition of high primary SNR. In addition, multi-user diversity technology can be also used to improve system performance. Furthermore, we also analyzed other parameters that influence the system performance to provide a better understanding of the secrecy of the cognitive IoT with EH.

Author Contributions: Conceptualization, P.X., F.L., I.Y., L.X. and H.W.; methodology, P.X. and I.Y.; software, P.X. and F.L.; validation, P.X., I.Y., H.W. and H.M.; formal analysis, P.X. and F.L.; investigation, I.Y. and H.M.; resources, P.X., I.Y., L.X. and H.W.; data curation, P.X., I.Y. and H.M.; writing—original draft preparation, P.X., F.L., I.Y. and L.X.; writing—review and editing, P.X., I.Y., H.W. and H.M.; visualization, P.X., F.L., I.Y., L.X., H.W. and H.M.; supervision, P.X. and I.Y.; project administration, P.X., I.Y. and H.W.; funding acquisition, P.X. and L.X. All authors have read and agreed to the published version of the manuscript.

Funding: This work is partially supported by the National Natural Science Foundation of China (NSFC) under Grants No. 61801171 and 62072158, in part by the Henan Province Science Fund for Distinguished Young Scholars (222300420006), and Program for Innovative Research Team in University of Henan Province (21IRTSTHN015), and in part by the Key Technologies R and D program of Henan Province under Grants no. 212102210168 and 222102210001.

Institutional Review Board Statement: Not applicable.

Informed Consent Statement: Not applicable.

Data Availability Statement: Not applicable.

Conflicts of Interest: The authors declare no conflict of interest.

Appendix A

From (27), by using (7) and letting $\Delta_P = 2^{\frac{R_P}{(1-\mu)^T}} - 1$, (27) is rewritten as

$$\begin{aligned} \Pr\{Q = \emptyset\} &= \prod_{i=1}^K \Pr\{C_{P2} < R_P\} = \prod_{i=1}^K \Pr\left\{\frac{P_{S_i}|h_{S_iD}|^2 + N_0}{P_P|h_P|^2} > \frac{1}{\Delta_P}\right\} \\ &= \prod_{i=1}^K \Pr\left\{\min\left(\frac{I}{|h_{S_iD}|^2}, \frac{\eta\mu P_P|h_{PS_i}|^2 + P_0}{1-\mu}\right)|h_{S_iD}|^2 + N_0 > \frac{P_P|h_P|^2}{\Delta_P}\right\} \\ &= \prod_{i=1}^K \left[\underbrace{\Pr\left\{\frac{I}{|h_{S_iD}|^2} \cdot |h_{S_iD}|^2 + N_0 > \frac{P_P|h_P|^2}{\Delta_P}\right\}}_{\text{Ch1}} \right. \\ &\quad \left. \times \underbrace{\Pr\left\{\frac{\eta\mu P_P|h_{PS_i}|^2 + P_0}{1-\mu} \cdot |h_{S_iD}|^2 + N_0 > \frac{P_P|h_P|^2}{\Delta_P}\right\}}_{\text{Ch2}} \right]. \end{aligned} \quad (\text{A1})$$

Here, $|h_{PS_i}|^2$, $|h_P|^2$, and $|h_{S_iD}|^2$ are independently and exponentially distributed random variables with parameters $1/\sigma_{PS_i}^2$, $1/\sigma_P^2$, and $1/\sigma_{S_iD}^2$, respectively. Let $X_1 = |h_{PS_i}|^2$, $X_2 = |h_P|^2$, and $X_3 = |h_{S_iD}|^2$, and their PDFs are given by (1). Thus, Ch1 can be derived as

$$\begin{aligned} \text{Ch1} &= \Pr\{I + N_0 > P_P X_2 / \Delta_P\} = 1 - \Pr\{I + N_0 < P_P X_2 / \Delta_P\} \\ &= 1 - \int_{\frac{\Delta_P I + \Delta_P N_0}{P_P}}^{\infty} \frac{1}{\sigma_P^2} e^{-\frac{x_2}{\sigma_P^2}} dx_2 = 1 - e^{-\frac{\Delta_P I + \Delta_P N_0}{P_P \sigma_P^2}}. \end{aligned} \quad (\text{A2})$$

Meanwhile, Ch2 can be derived as

$$\begin{aligned}
\text{Ch2} &= \Pr\left\{\frac{\eta\mu P_P X_1 X_3 + P_0 X_3}{1-\mu} + N_0 > \frac{P_P X_2}{\Delta_P}\right\} \\
&= 1 - \Pr\left\{\frac{\eta\mu P_P X_1 X_3 + P_0 X_3}{1-\mu} + N_0 < \frac{P_P X_2}{\Delta_P}\right\} \\
&= 1 - \int_0^\infty \frac{1}{\sigma_{S_iD}^2} e^{-\frac{x_3}{\sigma_{S_iD}^2}} dx_3 \int_0^\infty \frac{1}{\sigma_{P_Si}^2} e^{-\frac{x_1}{\sigma_{P_Si}^2}} dx_1 \int_0^\infty \frac{1}{\sigma_P^2} e^{-\frac{x_2}{\sigma_P^2}} dx_2 \\
&= 1 - \int_0^\infty \frac{1}{\sigma_{S_iD}^2} e^{-\frac{x_3}{\sigma_{S_iD}^2}} dx_3 \int_0^\infty \frac{1}{\sigma_{P_Si}^2} e^{-\frac{x_1}{\sigma_{P_Si}^2}} dx_1 \times e^{-\left(\frac{\eta\mu P_P x_3 x_1 + P_0 x_3}{(1-\mu)P_P} + \frac{\Delta_P N_0}{P_P}\right)} \\
&= 1 + \frac{(1-\mu)\sigma_P^2}{\eta\mu\sigma_{S_iD}^2\sigma_{P_Si}^2\Delta_P} e^{-\frac{N_0\Delta_P}{P_P\sigma_P^2} + \frac{(1-\mu)P_P\sigma_P^2 + \Delta_P P_0\sigma_{S_iD}^2}{\eta\mu\sigma_{S_iD}^2\sigma_{P_Si}^2\Delta_P P_P}} \times \text{Ei}\left(-\frac{(1-\mu)P_P\sigma_P^2 + \Delta_P P_0\sigma_{S_iD}^2}{\eta\mu\sigma_{S_iD}^2\sigma_{P_Si}^2\Delta_P P_P}\right), \tag{A3}
\end{aligned}$$

where $\text{Ei}(x) = \int_{-\infty}^x \frac{1}{u} e^u du = \gamma + \ln(-x) + \sum_{n=1}^{\infty} \frac{x^n}{n \cdot n!}$, $x < 0$, γ is the Euler's constant.

From (30), by using (7) and letting $\Delta_S = 2^{\frac{R_S}{(1-\mu)T}} - 1$ and $a_1 = \frac{|h_{S_i}|^2}{P_P|h_{PB}|^2 + N_0}$, (32) can be rewritten as

$$\begin{aligned}
&\Pr\{\Psi_S|Q = Q_i\} \\
&= \prod_{i=1}^L \left[1 - \Pr\left\{\min\left(\frac{I}{|h_{S_iD}|^2}, \frac{\eta\mu P_P |h_{P_Si}|^2 + P_0}{1-\mu}\right) a_1 > \Delta_S\right\}\right] \\
&= \prod_{i=1}^L \left[1 - \Pr\left\{\underbrace{\frac{|h_{S_i}|^2 \cdot I / |h_{S_iD}|^2}{P_P |h_{PB}|^2 + N_0}}_{\text{Ch3}} > \Delta_S\right\}\right. \\
&\quad \left. \times \Pr\left\{\underbrace{\frac{|h_{S_i}|^2 (\eta\mu P_P |h_{P_Si}|^2 + P_0) / (1-\mu)}{P_P |h_{PB}|^2 + N_0}}_{\text{Ch4}} > \Delta_S\right\}\right]. \tag{A4}
\end{aligned}$$

Here, $|h_{PB}|^2$ and $|h_{S_i}|^2$ are independently and exponentially distributed random variables with parameters $1/\sigma_{PB}^2$ and $1/\sigma_{S_i}^2$, respectively. Let $X_4 = |h_{PB}|^2$ and $X_5 = |h_{S_i}|^2$; their PDFs are given by (1). Let $Y_1 = X_5/X_3$; the PDF of variable Y_1 is derived in Appendix B from (A16). By using $f_{Y_1}(y_1)$, Ch3 can be derived as

$$\begin{aligned}
\text{Ch3} &= 1 - \Pr\{I \cdot W_1 < \Delta_S P_P X_4 + \Delta_S N_0\} \\
&= 1 - \int_0^\infty f_{Y_1}(y_1) dy_1 \int_{\frac{I y_1 - \Delta_S N_0}{\Delta_S P_P}}^\infty \frac{1}{\sigma_{PB}^2} e^{-\frac{x_4}{\sigma_{PB}^2}} dx_4 \\
&= 1 - e^{-\frac{N_0}{P_P\sigma_{PB}^2}} \int_0^\infty \frac{\sigma_{S_i}^2 \sigma_{S_iD}^2}{(\sigma_{S_i}^2 + \sigma_{S_iD}^2 y_1)^2} e^{-\frac{I}{\Delta_S P_P \sigma_{PB}^2} y_1} dy_1 \\
&= 1 - \frac{\sigma_{S_i}^2}{\sigma_{S_iD}^2} e^{\frac{N_0}{P_P\sigma_{PB}^2}} \left[\frac{I}{\Delta_S P_P \sigma_{PB}^2} e^{\frac{I\sigma_{S_i}^2}{\Delta_S P_P \sigma_{PB}^2 \sigma_{S_iD}^2}} \text{Ei}\left(\frac{-I\sigma_{S_i}^2}{\Delta_S P_P \sigma_{PB}^2 \sigma_{S_iD}^2}\right) + \frac{\sigma_{S_iD}^2}{\sigma_{S_i}^2} \right]. \tag{A5}
\end{aligned}$$

In addition, Ch4 can be derived as

$$\begin{aligned}
 \text{Ch4} &= 1 - \Pr \left\{ \frac{\eta\mu P_P X_5 X_1 + P_0 X_5}{1 - \mu} < (\Delta_S P_P X_4 + \Delta_S N_0) \right\} \\
 &= 1 - \int_0^\infty \frac{1}{\sigma_{S_i}^2} e^{-\frac{x_5}{\sigma_{S_i}^2}} dx_5 \int_0^\infty \frac{1}{\sigma_{PS_i}^2} e^{-\frac{x_1}{\sigma_{PS_i}^2}} dx_1 \int_0^\infty \frac{1}{\sigma_{PB}^2} e^{-\frac{x_4}{\sigma_{PB}^2}} dx_4 \\
 &= 1 - \frac{1}{\sigma_{S_i}^2} e^{\frac{N_0}{P_P \sigma_{PB}^2}} \int_0^\infty \frac{(1 - \mu) \Delta_S \sigma_{PB}^2}{(1 - \mu) \Delta_S \sigma_{PB}^2 + \eta\mu \sigma_{PS_i}^2 x_5} e^{-\frac{x_5}{\sigma_{S_i}^2} - \frac{P_0 x_5}{(1 - \mu) \Delta_S P_P \sigma_{PB}^2}} dx_5 \\
 &= 1 + \frac{(1 - \mu) \Delta_S \sigma_{PB}^2}{\eta\mu \sigma_{S_i}^2 \sigma_{PS_i}^2} e^{\left(\frac{1}{\sigma_{S_i}^2} + \frac{P_0}{(1 - \mu) \Delta_S P_P \sigma_{PB}^2} \right) \frac{(1 - \mu) \Delta_S \sigma_{PB}^2}{\eta\mu \sigma_{PS_i}^2} + \frac{N_0}{P_P \sigma_{PB}^2}} \\
 &\quad \times \text{Ei} \left[- \left(\frac{1}{\sigma_{S_i}^2} + \frac{P_0}{(1 - \mu) \Delta_S P_P \sigma_{PB}^2} \right) \frac{(1 - \mu) \Delta_S \sigma_{PB}^2}{\eta\mu \sigma_{PS_i}^2} \right].
 \end{aligned} \tag{A6}$$

From (36), let $X_6 = |h_{PE}|^2$, $X_7 = |h_{SE}|^2$, $X_8 = |h_{SE}|^2$, $X_9 = |h_{PS_n}|^2$, and the PDF of variable Y_2 is derived in Appendix B from (A16) to (A17). By using $f_{Y_2}(y_2)$, Ch5 and Ch6 can be derived as (A7) and (A8), respectively.

$$\begin{aligned}
 \text{Ch5} &= \Pr \left\{ IY_2 + \frac{\eta\mu P_P X_9 X_8}{1 - \mu} + N_0 > P_P X_6 / \Delta_P \right\} \\
 &= 1 - \int_0^\infty \frac{\sigma_{S_iE}^2 \sigma_{S_iD}^2}{(\sigma_{S_iE}^2 + \sigma_{S_iD}^2 y_2)^2} dy_2 \int_0^\infty \frac{1}{\sigma_{PS_n}^2} e^{-\frac{x_9}{\sigma_{PS_n}^2}} dx_9 \int_0^\infty \frac{1}{\sigma_{S_nE}^2} e^{-\frac{x_8}{\sigma_{S_nE}^2}} dx_8 \\
 &\quad \times \int_0^\infty \frac{1}{\sigma_{PE}^2} e^{-\frac{x_6}{\sigma_{PE}^2}} dx_6 \\
 &= 1 - \int_0^\infty \frac{\sigma_{S_iE}^2 \sigma_{S_iD}^2}{(\sigma_{S_iE}^2 + \sigma_{S_iD}^2 y_2)^2} dy_2 \int_0^\infty \frac{1}{\sigma_{PS_n}^2} e^{-\frac{x_9}{\sigma_{PS_n}^2}} dx_9 \int_0^\infty \frac{1}{\sigma_{S_nE}^2} e^{-\frac{x_8}{\sigma_{S_nE}^2}} dx_8 \\
 &\quad \times e^{-\left(\frac{\Delta_P I y_2}{P_P} + \frac{\eta\mu \Delta_P x_8 x_9}{1 - \mu} + \frac{N_0 \Delta_P}{P_P} \right)} \\
 &= 1 + \left\{ e^{-\frac{N_0 \Delta_P}{P_P \sigma_{PE}^2} + \frac{(1 - \mu) \sigma_{PE}^2}{\eta\mu \Delta_P \sigma_{S_nE}^2 \sigma_{PS_n}^2}} \frac{(1 - \mu) \sigma_{PE}^2}{\eta\mu \Delta_P \sigma_{S_nE}^2 \sigma_{PS_n}^2} \text{Ei} \left(- \frac{(1 - \mu) \sigma_{PE}^2}{\eta\mu \Delta_P \sigma_{S_nE}^2 \sigma_{PS_n}^2} \right) \right. \\
 &\quad \left. \times \frac{\sigma_{S_iE}^2}{\sigma_{S_iD}^2} \left[\frac{I \Delta_P}{P_P \sigma_{PE}^2} e^{\frac{I \Delta_P \sigma_{S_iE}^2}{P_P \sigma_{PE}^2 \sigma_{S_iD}^2}} \cdot \text{Ei} \left(\frac{-I \Delta_P \sigma_{S_iE}^2}{P_P \sigma_{PE}^2 \sigma_{S_iD}^2} \right) + \frac{\sigma_{S_iD}^2}{\sigma_{S_iE}^2} \right] \right\},
 \end{aligned} \tag{A7}$$

$$\begin{aligned}
 \text{Ch6} &= \Pr \left\{ \frac{(\eta\mu P_P X_1 + P_0)X_7 + \eta\mu P_P X_9 X_8}{1 - \mu} + N_0 > \frac{P_P X_6}{\Delta_P} \right\} \\
 &= 1 - \left[\int_0^\infty \frac{1}{\sigma_{S_n E}^2} e^{-\frac{x_8}{\sigma_{S_n E}^2}} \int_0^\infty \frac{1}{\sigma_{P S_n}^2} e^{-\frac{x_9}{\sigma_{P S_n}^2}} dx_9 dx_8 \int_0^\infty \frac{1}{\sigma_{P S_i}^2} e^{-\frac{x_1}{\sigma_{P S_i}^2}} \int_0^\infty \frac{1}{\sigma_{S_i E}^2} e^{-\frac{x_7}{\sigma_{S_i E}^2}} dx_7 dx_1 \right. \\
 &\quad \left. \times \int_0^\infty \frac{1}{\sigma_{P E}^2} e^{-\frac{x_6}{\sigma_{P E}^2}} dx_6 \right] \\
 &= 1 - \left[\int_0^\infty \frac{1}{\sigma_{S_n E}^2} e^{-\frac{x_8}{\sigma_{S_n E}^2}} \int_0^\infty \frac{1}{\sigma_{P S_n}^2} e^{-\frac{x_9}{\sigma_{P S_n}^2}} dx_9 dx_8 \int_0^\infty \frac{1}{\sigma_{P S_i}^2} e^{-\frac{x_1}{\sigma_{P S_i}^2}} \int_0^\infty \frac{1}{\sigma_{S_i E}^2} e^{-\frac{x_7}{\sigma_{S_i E}^2}} dx_7 dx_1 \right. \\
 &\quad \left. \times e^{-\left(\frac{P_0 \Delta_P x_7}{(1-\mu)P_P} + \frac{\eta\mu \Delta_P x_1 x_7}{1-\mu} + \frac{\eta\mu \Delta_P x_9 x_8}{1-\mu} + \frac{\Delta_P N_0}{P_P}\right)} \right] \tag{A8} \\
 &= 1 - \left\{ \left[\frac{(1-\mu)\sigma_{P E}^2}{\eta\mu \Delta_P} \right]^2 \frac{1}{\sigma_{P S_n}^2 \sigma_{P S_i}^2 \sigma_{S_i E}^2 \sigma_{S_n E}^2} e^{-\frac{N_0 \Delta_P}{P_P \sigma_{P E}^2} + \frac{P_0 \Delta_P \sigma_{S_i E}^2 + (1-\mu)P_P \sigma_{P E}^2}{\eta\mu \Delta_P P_P \sigma_{S_i E}^2 \sigma_{P S_i}^2} + \frac{(1-\mu)\sigma_{P E}^2}{\eta\mu \Delta_P \sigma_{P S_n}^2 \sigma_{S_n E}^2}} \right. \\
 &\quad \left. \times \text{Ei} \left[-\frac{P_0 \Delta_P \sigma_{S_i E}^2 + (1-\mu)P_P \sigma_{P E}^2}{\eta\mu \Delta_P P_P \sigma_{S_i E}^2 \sigma_{P S_i}^2} \right] \text{Ei} \left[-\frac{(1-\mu)\sigma_{P E}^2}{\eta\mu \Delta_P \sigma_{P S_n}^2 \sigma_{S_n E}^2} \right] \right\}.
 \end{aligned}$$

By using (16), (41) can be rewritten as,

$$\begin{aligned}
 \Pr \{ Q^{OSTS} = \emptyset \} &= \prod_{i=1}^K \Pr \{ C_{P2}^{OSTS} < R_P \} = \prod_{i=1}^K \Pr \left\{ \frac{\xi P_{S_i}^{OSTS} |h_{S_i D}|^2 + N_0}{P_P |h_P|^2} > \frac{1}{\rho_P} \right\} \\
 &= \prod_{i=1}^K \Pr \left\{ \min \left(\frac{I}{|h_{S_i D}|^2}, P_0 \right) \cdot \xi |h_{S_i D}|^2 + N_0 > \frac{P_P |h_P|^2}{\rho_P} \right\} \\
 &= \prod_{i=1}^K \left[\underbrace{\Pr \left\{ \frac{\xi I}{|h_{S_i D}|^2} \cdot |h_{S_i D}|^2 + N_0 > \frac{P_P |h_P|^2}{\rho_P} \right\}}_{\text{Ch7}} \right. \\
 &\quad \left. \times \underbrace{\Pr \left\{ \xi P_0 \cdot |h_{S_i D}|^2 + N_0 > \frac{P_P |h_P|^2}{\rho_P} \right\}}_{\text{Ch8}} \right]. \tag{A9}
 \end{aligned}$$

Hence, Ch7 is derived as

$$\begin{aligned}
 \text{Ch7} &= \Pr \{ \xi I + N_0 > P_P X_2 / \rho_P \} = 1 - \Pr \{ \xi I + N_0 < P_P X_2 / \rho_P \} \\
 &= 1 - \int_{\frac{\rho_P \xi I + \rho_P N_0}{P_P}}^\infty \frac{1}{\sigma_P^2} e^{-\frac{x_2}{\sigma_P^2}} dx_2 = 1 - e^{-\frac{\rho_P \xi I + \rho_P N_0}{P_P \sigma_P^2}}. \tag{A10}
 \end{aligned}$$

Ch8 can be derived as follows:

$$\begin{aligned}
 \text{Ch8} &= \Pr\{\zeta P_0 X_3 + N_0 > P_P X_2 / \rho_P\} = 1 - \Pr\{\zeta P_0 X_3 + N_0 < P_P X_2 / \rho_P\} \\
 &= 1 - \int_0^\infty \frac{1}{\sigma_{S_iD}^2} e^{-\frac{x_3}{\sigma_{S_iD}^2}} dx_3 \int_{\frac{\zeta P_0 x_3 \rho_P}{P_P} + \frac{\rho_P N_0}{P_P}}^\infty \frac{1}{\sigma_P^2} e^{-\frac{x_2}{\sigma_P^2}} dx_2 \\
 &= 1 - \int_0^\infty \frac{1}{\sigma_{S_iD}^2} e^{-\frac{x_3}{\sigma_{S_iD}^2}} dx_3 \times e^{-\left(\frac{\zeta P_0 x_3 \rho_P}{P_P} + \frac{\rho_P N_0}{P_P}\right)} \\
 &= 1 + \frac{P_P \sigma_P^2}{P_P \sigma_P^2 + \rho_P \zeta P_0 \sigma_{S_iD}^2} e^{-\frac{N_0 \rho_P}{P_P \sigma_P^2}}.
 \end{aligned} \tag{A11}$$

From (44), we can obtain

$$\begin{aligned}
 \text{Ch9} &= 1 - \Pr\{\zeta I Y_1 / (P_P \rho_S) - N_0 / P_P < X_4\} \\
 &= 1 - \int_0^\infty \frac{\sigma_{S_i}^2 \sigma_{S_iD}^2}{\left(\sigma_{S_i}^2 + \sigma_{S_iD}^2 y_1\right)^2} dy_1 \int_{\frac{\zeta I y_1}{P_P \rho_S} - \frac{N_0}{P_P}}^\infty \frac{1}{\sigma_{PB}^2} e^{-\frac{x_4}{\sigma_{PB}^2}} dx_4 \\
 &= 1 - \int_0^\infty \frac{\sigma_{S_i}^2 \sigma_{S_iD}^2}{\left(\sigma_{S_i}^2 + \sigma_{S_iD}^2 y_1\right)^2} dy_1 \times e^{-\left(\frac{\zeta I y_1}{P_P \rho_S} - \frac{N_0}{P_P}\right)} \\
 &= 1 - \frac{\sigma_{S_i}^2}{\sigma_{S_iD}^2} e^{-\frac{N_0}{P_P \sigma_{PB}^2}} \left[\frac{\zeta I}{\rho_S P_P \sigma_{PB}^2} e^{\frac{\rho_S P_P \sigma_{PB}^2 \zeta I}{\sigma_{S_iD}^2}} \times \text{Ei}\left(-\frac{\zeta I \sigma_{S_i}^2}{\rho_S P_P \sigma_{PB}^2 \sigma_{S_iD}^2}\right) + \frac{\sigma_{S_iD}^2}{\sigma_{S_i}^2} \right],
 \end{aligned} \tag{A12}$$

$$\text{Ch10} = \Pr\left\{X_5 > \frac{P_P \rho_S X_4 + \rho_S N_0}{\zeta P_0}\right\} = \frac{\zeta P_0 \sigma_{S_i}^2 e^{-\rho_S N_0 / (P_0 \sigma_{S_i}^2)}}{\zeta P_0 \sigma_{S_i}^2 + P_P \rho_S \sigma_{PB}^2}. \tag{A13}$$

Considering $Y_2 = |h_{S_iE}|^2 / |h_{S_iD}|^2$, then using the PDF of Y_2 , which is calculated in Appendix B, from (46), we can obtain

$$\begin{aligned}
 \text{Ch11} &= \Pr\left\{P_P |h_{PE}|^2 < \rho_P \left(|h_{S_iE}|^2 / |h_{S_iD}|^2 + N_0\right)\right\} \\
 &= \int_0^\infty \frac{\sigma_{S_iE}^2 \sigma_{S_iD}^2}{\left(\sigma_{S_iE}^2 + \sigma_{S_iD}^2 y_2\right)^2} dy_2 \int_0^{\frac{I \rho_P y_2}{P_P} + \frac{\rho_P N_0}{P_P}} \frac{1}{\sigma_{PE}^2} e^{-\frac{x_6}{\sigma_{PE}^2}} dx_6 \\
 &= 1 - \frac{\sigma_{S_iE}^2}{\sigma_{S_iD}^2} e^{-\frac{\rho_P N_0}{P_P \sigma_{PE}^2}} \left[\frac{I \rho_P}{P_P \sigma_{PE}^2} e^{\frac{I \rho_P \sigma_{S_iE}^2}{P_P \sigma_{PE}^2 \sigma_{S_iD}^2}} \times \text{Ei}\left(-\frac{I \rho_P \sigma_{S_iE}^2}{P_P \sigma_{PE}^2 \sigma_{S_iD}^2}\right) + \frac{\sigma_{S_iD}^2}{\sigma_{S_iE}^2} \right],
 \end{aligned} \tag{A14}$$

$$\text{Ch12} = \Pr\left\{\frac{P_P |h_{PE}|^2}{P_0 |h_{S_iE}|^2 + N_0} < \rho_P\right\} = 1 - \frac{P_P \sigma_{PE}^2 e^{-\rho_P N_0 / (P_P \sigma_{PE}^2)}}{P_P \sigma_{PE}^2 + P_0 \rho_P \sigma_{S_iE}^2}. \tag{A15}$$

Appendix B

According to $X_5 = |h_{S_i}|^2$, $X_3 = |h_{S_iD}|^2$, and (1), let $Y_1 = X_5/X_3$; then, the PDF of Y_1 can be derived as

$$\begin{aligned} F_{Y_1}(y_1) &= \Pr\left\{\frac{X_5}{X_3} < y_1\right\} \\ &= \int_0^\infty \frac{1}{\sigma_{S_iD}^2} e^{-\frac{x_3}{\sigma_{S_iD}^2}} \int_0^{x_4 y_1} \frac{1}{\sigma_{S_i}^2} e^{-\frac{x_5}{\sigma_{S_i}^2}} dx_5 dx_3 \\ &= 1 - \sigma_{S_i}^2 / \left(\sigma_{S_i}^2 + \sigma_{S_iD}^2 y_1\right) \\ &\Rightarrow f_{Y_1}(y_1) = \sigma_{S_iD}^2 \sigma_{S_i}^2 / \left(\sigma_{S_i}^2 + \sigma_{S_iD}^2 y_1\right)^2. \end{aligned} \quad (A16)$$

Let $Y_2 = X_7/X_3$, where $X_7 = |h_{S_iE}|^2$. Similar to the derivation of the PDF of Y_1 , the PDF of Y_2 can be obtained by (A17).

$$f_{Y_2}(y_2) = \sigma_{S_iD}^2 \sigma_{S_iE}^2 / \left(\sigma_{S_iE}^2 + \sigma_{S_iD}^2 y_2\right)^2. \quad (A17)$$

References

- McMahan, H.B.; Moore, E.; Ramage, D.; Hampson, S.; Arcas, B.A.Y. Communication-efficient learning of deep networks from decentralized data. In Proceedings of the 20th International Conference on Artificial Intelligence and Statistics (AISTATS), Lauderdale, FL, USA, 20–22 April 2017; pp. 1273–1282.
- Song, F.; Zhu, M.; Zhou, Y.; You, I.; Zhang, H. Smart collaborative tracking for ubiquitous power iot in edge-cloud interplay domain. *IEEE Internet Things J.* **2020**, *7*, 6046–6055.
- Song, F.; Li, L.; You, I.; Zhang, H. Enabling heterogeneous deterministic networks with smart collaborative theory. *IEEE Network.* **2021**, *35*, 64–71.
- Mitola, J. *Cognitive Radio: An Integrated Agent Architecture for Software Defined Radio*; K Thesis Royal Institute of Technology: Stockholm, Sweden, 2000.
- Haykin, S. Cognitive radio: Brain-empowered wireless communications. *IEEE J. Select. Areas Commun.* **2005**, *23*, 201–220.
- Goldsmith, A.; Jafar, S.A.; Maric, I.; Srinivasa, S. Breaking spectrum gridlock with cognitive radios: An information theoretic perspective. *Proc. IEEE* **2009**, *97*, 894–914.
- Song, F.; Ai, Z.; Zhou, Y.; You, I.; Choo, K.-K.R.; Zhang, H. Smart collaborative automation for receive buffer control in multipath industrial networks. *IEEE Trans. Ind. Inform.* **2020**, *16*, 1385–1394.
- Song, F.; Ai, Z.; Zhang, H.; You, I.; Li, S. Smart collaborative balancing for dependable network components in cyber-physical systems. *IEEE Trans. Ind. Inform.* **2021**, *17*, 6916–6924.
- Li, J.; Feng, Z.; Feng, Z.; Zhang, P. A survey of security issues in cognitive radio networks. *China Commun.* **2015**, *12*, 132–150.
- Xie, N.; Chen, C.; Ming, Z. Security model of authentication at the physical layer and performance analysis over fading channels. *IEEE Trans. Depend. Secure Comput.* **2021**, *18*, 253–268.
- Sharma, R.K.; Rawat, D.B. Advances on security threats and countermeasures for cognitive radio networks: A survey. *IEEE Commun Surv. Tutorials* **2015**, *17*, 1023–1043.
- Nguyen, V.-D.; Hoang, T.M.; Shin, O.-S. Secrecy capacity of the primary system in a cognitive radio network. *IEEE Trans. Veh. Technol.* **2015**, *64*, 3834–3843.
- Csiszar, I.; Korner, J. Broadcast channels with confidential messages. *IEEE Trans. Inform. Theory* **1978**, *24*, 339–348.
- Tang, X.; Liu, R.; Spasojevic, P.; Poor, H.V. The Gaussian wiretap channel with a helping interferer. In Proceedings of the 2008 IEEE International Symposium on Information Theory, Toronto, ON, Canada, 6–11 July 2008; pp. 389–393.
- Oggier, F.; Hassibi, B. The secrecy capacity of the MIMO wiretap channel. In Proceedings of the 2008 IEEE International Symposium on Information Theory, Toronto, ON, Canada, 6–11 July 2008; pp. 524–528.
- Lei, H.; Gao, C.; Ansari, I.S.; Guo, Y.; Zou, Y.; Pan, G.; Qaraqe, K.A. Secrecy outage performance of transmit antenna selection for MIMO underlay cognitive radio systems over nakagami- m channels. *IEEE Trans. Veh. Technol.* **2017**, *66*, 2237–2250.
- Wu, Y.; Schober, R.; Ng, D.W.K.; Xiao, C.; Caire, G. Secure massive MIMO transmission with an active eavesdropper. *IEEE Trans. Inform. Theory* **2016**, *62*, 3880–3900.
- Wang, C.; Wang, H.-M. On the secrecy throughput maximization for MISO cognitive radio network in slow fading channels. *IEEE Trans. Inform. Forens. Secur.* **2014**, *9*, 1814–1827.
- Gong, C.; Yue, X.; Zhang, Z.; Wang, X.; Dai, X.. Enhancing physical layer security with artificial noise in large-scale NOMA networks. *IEEE Trans. Veh. Technol.* **2021**, *70*, 2349–2361.

20. Perazzone, J.B.; Yu, P.L.; Sadler, B.M.; Blum, R.S. Artificial noise-aided MIMO physical layer authentication with imperfect CSI. *IEEE Trans. Inform. Forens. Secur.* **2021**, *16*, 2173–2185.
21. Li, B.; Zou, Y.; Zhou, J.; Wang, F.; Cao, W.; Yao, Y.-D. Secrecy outage probability analysis of friendly jammer selection aided multiuser scheduling for wireless networks. *IEEE Trans. Commun.* **2019**, *67*, 3482–3495.
22. Wang, L.; Sheng, M.; Zhang, Y.; Wang, X.; Xu, C. Robust energy efficiency maximization in cognitive radio networks: The worst-case optimization approach. *IEEE Trans. Commun.* **2015**, *63*, 51–65.
23. Mili, M.R.; Musavian, L.; Hamdi, K.A.; Marvasti, F. How to increase energy efficiency in cognitive radio networks. *IEEE Trans. Commun.* **2016**, *64*, 1829–1843.
24. Ozcan, G.; Gursoy, M.C.; Tang, J.. Spectral and energy efficiency in cognitive radio systems with unslotted primary users and sensing uncertainty. *IEEE Trans. Commun.* **2017**, *65*, 4138–4151.
25. Li, D.; Cheng, J.; Leung, V.C.M.. Adaptive spectrum sharing for half-duplex and full-duplex cognitive radios: From the energy efficiency perspective. *IEEE Trans. Commun.* **2018**, *66*, 5067–5080.
26. Mamaghani, M.T.; Kuhestani, A.; Wong, K.-K. Secure two-way transmission via wireless-powered untrusted relay and external jammer. *IEEE Trans. Veh. Technol.* **2018**, *67*, 8451–8465.
27. Ren, J.; Hu, J.; Zhang, D.; Guo, H.; Zhang, Y.; Shen, X. RF energy harvesting and transfer in cognitive radio sensor networks: Opportunities and challenges. *IEEE Commun. Mag.* **2018**, *56*, 104–110.
28. Jiang, X.; Li, P.; Li, B.; Zou, Y.; Wang, R. Secrecy performance of transmit antenna selection for underlay MIMO cognitive radio relay networks with energy harvesting. *IET Commun.* **2022**, *16*, 227–245.
29. Le, T.-D.; Shin, O.-S. Wireless energy harvesting in cognitive radio with opportunistic relays selection. In Proceedings of the 2015 IEEE 26th Annual International Symposium on Personal, Indoor, and Mobile Radio Communications (PIMRC), Hong Kong, China, 30 August–2 September 2015; pp. 949–953.
30. Nguyen, V.-D.; Dinh-Van, S.; Shin, O.-S. Opportunistic relaying with wireless energy harvesting in a cognitive radio system. In Proceedings of the 2015 IEEE Wireless Communications and Networking Conference (WCNC), New Orleans, LA, USA, 9–12 March 2015; pp. 87–92.
31. Zheng, K.; Liu, X.; Zhu, Y.; Chi, K.; Liu, K. Total throughput maximization of cooperative cognitive radio networks with energy harvesting. *IEEE Transactions Wirel. Commun.* **2020**, *19*, 533–546.
32. Liu, X.; Zheng, K.; Chi, K.; Zhu, Y.-H. Cooperative spectrum sensing optimization in energy-harvesting cognitive radio networks. *IEEE Trans. Wirel. Commun.* **2020**, *19*, 7663–7676.
33. Hong, T.M.; Duong, T.Q.; Vo, N.; Kundu, C. Physical Layer Security in Cooperative Energy Harvesting Networks With a Friendly Jammer. *IEEE Wirel. Commun. Lett.* **2017**, *6*, 174–177.
34. Ding, X.; Zou, Y.; Zhang, G.; Wang, X.C.X.; Hanzo, L. The Security–Reliability Tradeoff of Multiuser Scheduling-Aided Energy Harvesting Cognitive Radio Networks. *IEEE Trans. Commun.* **2019**, *67*, 3890–3904.
35. Yan, P.; Zou, Y.; Ding, X.; Zhu, J. Energy-Aware Relay Selection Improves Security-Reliability Tradeoff in Energy Harvesting Cooperative Cognitive Radio Systems. *IEEE Trans. Veh. Technol.* **2020**, *69*, 5115–5128.
36. Yan, P.; Zou, Y.; Zhu, J. Energy-aware multiuser scheduling for physical-layer security in energy-harvesting underlay cognitive radio systems. *IEEE Trans. Veh. Technol.* **2018**, *67*, 2084–2096.
37. Liu, Y.; Mousavifar, S.A.; Deng, Y.; Leung, C.; Elkashlan, M. Wireless energy harvesting in a cognitive relay network. *IEEE Trans. Wirel. Commun.* **2016**, *15*, 2498–2508.
38. Xie, P.; Zhu, J.; Zhang, M.; Xing, L.; Wu, H. Aided opportunistic jammer selection for secrecy improvement in underlay cognitive radio networks. *Wirel. Person. Commun.* **2019**, *107*.
39. Zou, Y.; Champagne, B.; Zhu, W.-P.; Hanzo, L. Relay-selection improves the security-reliability trade-off in cognitive radio systems. *IEEE Trans. Commun.* **2015**, *63*, 215–228.
40. El-Malek, A.H.A.; Salhab, A.M.; Zummo, S.A.; Alouini, M.-S. Security-reliability trade-off analysis for multiuser SIMO mixed RF/FSO relay networks with opportunistic user scheduling. *IEEE Trans. Wirel. Commun.* **2016**, *15*, 5904–5918.
41. Al-Hraishawi, H.; Baduge, G.A.A. Wireless Energy Harvesting in Cognitive Massive MIMO Systems With Underlay Spectrum Sharing. *IEEE Wirel. Commun. Lett.* **2017**, *6*, 134–137.